HHS Public Access

Author manuscript

Nat Commun. Author manuscript; available in PMC 2015 May 27.

Published in final edited form as:

Nat Commun. ; 5: 5583. doi:10.1038/ncomms6583.

FGF signaling specifies hematopoietic stem cells through its regulation of somitic Notch signaling

Yoonsung Lee[1], **Jennifer E Manegold**[1], **Albert D Kim**[1], **Claire Pouget**[1], **David L Stachura**[1,2], **Wilson K Clements**[1,3], and **David Traver**[1]

[1]Department of Cellular and Molecular Medicine and Section of Cell and Developmental Biology, University of California, San Diego, La Jolla, CA 92093. USA

[2]Department of Biological Sciences, California State University, Chico, CA 95929. USA

[3]Department of Hematology, St. Jude Children's Research Hospital, Memphis, TN, 38105. USA

Abstract

Hematopoietic stem cells (HSCs) derive from hemogenic endothelial cells of the primitive dorsal aorta (DA) during vertebrate embryogenesis. The molecular mechanisms governing this unique endothelial to hematopoietic transition remain unclear. Here, we demonstrate a novel requirement for fibroblast growth factor (FGF) signaling in HSC emergence. This requirement is non-cell-autonomous, and acts within the somite to bridge the Wnt and Notch signaling pathways. We previously demonstrated that Wnt16 regulates the somitic expression of two Notch ligands, *deltaC* (*dlc*) and *deltaD* (*dld*), whose combined function is required for HSC fate. How Wnt16 connects to Notch function has remained an open question. Our current studies demonstrate that FGF signaling, via FGF receptor 4 (Fgfr4), mediates a signal transduction pathway between Wnt16 and Dlc, but not Dld, to regulate HSC specification. Our findings demonstrate that FGF signaling acts as a key molecular relay within the developmental HSC niche to instruct HSC fate.

Keywords

FGF; hematopoietic stem cells; somites; Wnt16; DeltaC; fgfr4

INTRODUCTION

Vertebrate hematopoiesis initiates sequentially with primitive and definitive waves of blood cell production during embryogenesis[1–3]. Of these embryonic blood precursors, only HSCs persist into adulthood and are responsible for lifelong replenishment of the hematopoietic

Corresponding Author: David Traver, Tel: (858) 822-4593, Fax: (858) 822-5740, dtraver@ucsd.edu.

Author contributions

Y.L. designed the experiments, D.T. supervised the experiments., Y.L., J.E.M. and A.D.K. performed experiments, Y.L., C.P. and D.L.D analyzed the data and, Y.L., W.K.C. and D.T. wrote the manuscript.

Competing Financial Interests

The authors declare no competing financial interests.

system. In all vertebrate animals studied, HSCs arise from hemogenic endothelium in the floor of the DA[4,5]. Our current understanding of HSC formation suggests that this endothelial to hematopoietic transition (EHT), which occurs during a limited window in embryonic development, gives rise to the entire pool of HSCs for the life of the organism. A major goal of regenerative medicine is to replicate the development of HSCs *in vitro* from human pluripotent precursors. Despite decades of effort, this goal has not been achieved. A better understanding of the molecular cues utilized by the embryo to pattern HSCs from mesodermal precursors could inform these approaches.

Development of HSCs requires complex interactions between diverse molecular signaling pathways and downstream intracellular transduction networks. These pathways include Hedgehog signaling, which is required for development of endothelial progenitors and HSCs[6–8], Vascular endothelial growth factor (Vegf) signaling, which is critical for vasculogenesis and HSC specification[9–11], Bone morphogenetic protein (BMP) signaling, which specifies vascular cells from mesoderm[12,13], and Notch signaling, which is essential for HSC generation from hemogenic endothelial cells[14–16]. The FGF signaling pathway has likewise been shown to be important in mesoderm formation[17,18] and vasculogenesis[19,20], but only a handful of studies have addressed the role of FGF signaling in the development of the hematopoietic lineages.

FGF signaling has been demonstrated to regulate formation of primitive hematopoietic cells by negatively regulating erythroid gene expression in *Xenopus*[21]. In the avian system, FGFs block primitive erythroid differentiation and promote endothelial development[22]. In contrast, Fgf21 knockdown in zebrafish reduced the formation of erythroid and myeloid cells[23]. *In vitro* studies indicated that FGFs induced myeloid proliferation in human bone marrow cultures[24]. Although the role of FGF signaling in primitive hematopoiesis has been reasonably well studied, its contribution to definitive HSC formation has never been addressed. Studies of FGF signaling and HSCs in adult mice indicate that long-term repopulating HSCs are found exclusively within an FGFR1-expressing population, and that ectopic provision of FGF1 can stimulate the *in vitro* expansion of HSCs[25]. However, recent *in vivo* studies showed that FGFR1 is not required for the homeostasis of adult HSCs but rather in the recovery of hematopoiesis following injury by enhancing HSC proliferation[26].

In this study, we utilized transgenic zebrafish in which FGF signaling can be inducibly blocked[27]. Loss of FGF signaling during early somitogenesis stages led to a loss of HSCs without disrupting development of primitive hematopoiesis or endothelium. During the temporal knockdown window, the FGF target genes *pea3* and *erm*, as well as the receptors *fgfr1* and *fgfr4*, were expressed in somites but not in posterior lateral mesoderm (PLM), which includes HSC precursors. Expression of *pea3* and *fgfr4* was reduced following Wnt16 knockdown, which we previously showed is required for HSC emergence by its regulation of the Notch ligands *dlc* and *dld* in the developing somites[28]. Epistasis experiments demonstrated that ectopic activation of FGF signaling could rescue HSC specification in *wnt16* morphants. Within the somite, FGF signaling is therefore required downstream of Wnt16 function for HSC development. Blockade of FGF signaling led to loss of *dlc* expression, but did not alter *dld* expression. Loss of HSCs following ablation of FGF signaling was restored by ectopic Notch activation. More specifically, overexpression of *dlc*

mRNA rescued HSC emergence following loss of FGF signaling, demonstrating that FGF function is required for HSC emergence through its regulation of *dlc* expression. Finally, disappearance of HSCs following knockdown of Fgfr4 indicated that this receptor acts as a specific relay between Wnt16 and Dlc in the somite. Taken together, these results refine our understanding of the signaling cascades necessary within the somite to instruct HSC fate in the neighboring PLM, and should inform studies seeking the cues necessary to pattern HSCs *in vitro* from pluripotent precursors.

RESULTS

FGF signaling is required for HSC specification

In order to examine a potential role for FGF signaling in HSC development, we used transgenic zebrafish in which FGF signaling can be conditionally abrogated by heat-shock induction of a dominant-negative Fgfr1-EGFP fusion protein (*hsp70:dn-fgfr1*)[27]. To induce dominant-negative Fgfr1, we administered heat-shocks to transgenic animals during several different windows of development. Experimentally perturbed and wild-type (wt) embryos were examined from the outcrossed progeny of heterozygous *hsp70:dn-fgfr1* fish and wt animals, resulting in 50% transgenic and 50% wt controls. Because FGF signaling is critical for early vertebrate development including mesodermal patterning and somitogenesis[29,30], early induction of the *dn-fgfr1* transgene before 10 hours post fertilization (hpf) led to gross embryonic defects (Supplementary Fig. 1a). However, heat-induction during somitogenesis at 12 hpf (5 somites) using optimized heat-shock conditions (38°C, 20 min) led to robust and specific loss of HSCs (Fig. 1a–d; Supplementary Fig. 1c). Whole-mount *in situ* hybridization (WISH) with the definitive HSC markers *runx1* and *cmyb*[31–33] indicated that inhibition of FGF signaling at 12 hpf led to a near complete loss of *runx1* expression at 26 hpf and *cmyb* at 35 hpf, when compared to wt animals (Fig. 1a–d). Interestingly, more than 50% of *hsp70:dn-fgfr1* transgenic embryos induced at 12 hpf showed robust loss of *runx1* expression, whereas blockade of FGF signaling at 15 hpf (10 somites) or 17 hpf (15 somites) showed little alteration in *runx1* expression (Fig. 1e). Quantitative RT-PCR (qPCR) using 26 hpf wt and hsp70:dn-fgfr1 transgenic embryos showed that runx1 expression was reduced in the absence of Fgf signaling at 12 hpf (Supplementary Fig. 1b). This blockade of FGF signaling at 12 hpf yielded no alteration in the number of somites during somitogenesis (Supplementary Fig. 2h, i), and runx1 expression in hsp70:dn-fgfr1 transgenic embryos was similarly reduced at later developmental stages (comparing 30 hpf embryos to 26 hpf embryos; Supplementary Fig. 1d), suggesting that loss of HSCs following FGF blockade was not caused by aberrant developmental rate. We further quantified the number of *cmyb*$^{+}$ HSCs in the DA (yellow arrowheads in Figure 1c, d) and observed that FGF signaling inhibition at 12 hpf, but not at later time points, perturbed HSC formation, consistent with our *runx1* analyses (Fig. 1f). Further quantification of emerging HSCs using triple transgenic cmyb:GFP; kdrl:RFP; hsp70:dn-fgfr1 embryos demonstrated that cmyb+ kdrl+ double positive HSCs were significantly reduced after heat-induction at 12 hpf compared to wt (Fig. 1g–i). Additionally, at 4 and 5 dpf, expression of cmyb and rag1, markers of developing T lymphocytes in the thymus was largely lost following the ablation of FGF signaling at 12 hpf (Fig. 1j–m). Since thymocyte production requires upstream HSCs, these results indicate that FGF signaling is required for HSC development.

To more precisely determine the critical time window that FGF signaling affects HSC formation, we investigated the expression of dominant-negative Fgfr1-EGFP fusion proteins by confocal microscopy. Membrane-localized EGFP was observed within an hour of heat-shock (Fig. 1n, o), and robustly expressed by 3 hours (Fig. 1p). In parallel, we also examined expression of a known target of FGF signaling, *pea3*[34,35] (Fig. 1q). Concomitant with the expression of dominant negative Fgfr1-EGFP fusion protein, *pea3* expression was severely reduced at 2 hours post heat-shock (hpHS), and absent by 3 hpHS. Taken together, these data indicate that the temporal developmental window where FGF signaling is required to specify HSCs is during mid-somitogenesis between 14 and 17 hpf.

To determine whether failure of HSC specification in induced *hsp70:dn-fgfr1* animals was due to incorrect specification of other mesodermal tissues, we examined expression of the PLM markers *scl*, *fli1* and *lmo2* at 15 hpf (Fig. 2a, b; Supplementary Fig. 2a, b), the ventral mesoderm marker *cdx4* (Fig. 2c, d), the notochord marker shh and its targets ptc1 and ptc2 (Fig. 2e, f; Supplementary Fig. 2c, d), the somitic markers *desma* and *vegfa* (Fig. 2g, h; Supplementary Fig. 2g), and the primitive erythrocyte marker, *gata1* (Fig 2k, l), and a pan-leukocyte marker, *l-plastin* (Fig. 2m, n). We observed no gross alterations in any of these tissues or cells. Similarly, convergence of pre-hematopoietic mesoderm was not significantly affected (Fig. 2i, j). Importantly, expression of the pan-vascular markers kdrl, fli1 and cdh5 were normal at 26 hpf (Fig. 2o–r: Supplementary Fig. 2f, k), as was efnb2a, a marker of aortic fate commitment (Fig. 2s, t; Supplementary Fig. 2k), indicating that the observed HSC defects are not likely a result of improper aortic specification.

FGF signaling is active in the somites but not in the PLM

Upon refining the temporal window in which FGF signaling was required for HSC specification, we investigated what tissues were receiving FGF signals in this time frame to determine whether or not HSC specification might require FGFs cell-autonomously. First, we examined expression of the FGF targets *pea3* and *erm* at 15 hpf and observed that their expression localized mainly to somites (Supplementary Fig. 3). To more precisely determine the expression pattern of FGF target genes, we utilized two-color enzymatic or fluorescence WISH (FISH) using *pea3* and *erm* along with markers of PLM, which contains the precursors of HSCs[5,36–38] (Fig. 3a, d–f). Expression of *pea3* and *erm* was restricted primarily to the somites and pre-somitic mesoderm, and did not overlap with *fli1*$^{+}$ or *lmo2*$^{+}$ PLM at 15 hpf, indicating that FGF signaling required for HSC specification is active in somites but not in the pre-endothelial mesoderm.

Since FGF signaling is transduced by dimerized ligand-bound FGFRs[39], identifying the spatial distribution of individual receptors provides excellent resolution as to which cells are experiencing FGF signaling in addition to the expression of FGF targets. We examined the expression of all four FGFRs at 15 hpf utilizing WISH and observed no receptor expression in the PLM (Supplementary Fig. 3). In particular, *fgfr2* and *fgfr3* were not expressed in the embryo posterior, whereas *fgfr1* and *fgfr4* were expressed in the posterior somites, similar to the FGF targets *pea3* and *erm*. Two-color WISH using probes against *fgfr1* or *fgfr4* and the PLM marker *fli1* or *lmo2* also demonstrated that neither receptor was expressed in the *fli1*$^{+}$ or *lmo2*$^{+}$ PLM tissue (Fig. 3b, c, g–l). In addition to whole animal imaging approaches, we

purified PLM precursors (*fli1*$^{+}$) and somitic cells (*α-actin*$^{+}$) from 17 hpf *fli1:EGFP* or *α-actin:GFP* transgenic embryos by fluorescence-activated cell sorting (FACS), to query expression of *fgfr1* and *fgfr4* by qPCR. Consistent with our WISH and FISH results, expression of *fgfr1* and *fgfr4* segregated to the somite fractions (Fig. 3m, n). Taken together, these data suggest that FGF signaling does not act directly on HSC precursors and the requirements for FGF signaling is non-cell autonomous.

Wnt16 acts upstream of FGF signaling in HSC specification

Recent studies from our laboratory showed that Wnt16 regulates the somitic expression of the Notch ligands *dlc* and *dld* whose combined activity are required to specify HSCs during somitogenesis[28] (Supplementary Fig. 5a). Based on spatiotemporal similarities between Wnt16 and FGF activity, we hypothesized the existence of a Wnt16/FGF regulatory network in the somite between 14 and 17 hpf. To test this hypothesis, we first examined the expression of *wnt16* and the FGF target *pea3*. As we have seen previously28, wnt16 transcript was localized to a relatively anterior-dorsal-lateral compartment of each of the more rostral somites. pea3 was expressed in the anterior-lateral compartment of more posterior somites, as well as the presomitic mesoderm (Fig. 4a–e). As the perdurance and signaling range of Wnt16 protein is unknown, it is difficult to determine whether Wnt16 has a role in somitic maintenance of pea3 expression that initiates in the PSM. To further analyze potential epistasis between Wnt16 and FGFs, we knocked down *wnt16* with an antisense-morpholino (wnt16-MO) and assessed *pea3* expression (Fig. 4f, g; Supplementary fig. 4a). Expression of *pea3* was robustly downregulated in the formed somites at 17 hpf in the absence of Wnt16, although PSM expression was unaffected. These results indicate that Wnt16 regulates somitic FGF signaling within our noted HSC specification time window. Furthermore, expression of *fgfr4* was reduced in *wnt16* morphants, while *fgfr1* was unchanged relative to control embryos (Fig. 4h, i; Supplementary Fig. 4, 5a). To confirm that Wnt16 acts upstream of FGF signaling to specify HSCs, we utilized a heat-inducible gain-of-function animal carrying a constitutively-active Fgfr1 transgene (*hsp70:ca-fgfr1*)[40]. Ectopic activation of FGF signaling at 12 hpf recovered normal *runx1* expression in the DA at 26 hpf, as well as *pea3* expression at 17 hpf in *wnt16* morphants (Fig. 4j–n; Supplementary Fig. 5b). Uninjected but heat-shocked *hsp70:ca-fgfr1* animals showed no ectopic increase in *runx1* expression (Fig. 4k). Similar to the early somitic requirements for Wnt16 and FGF in HSC specification, Vegf signaling is known to function in the development of the vasculature and definitive HSCs during somitogenesis9–11. To determine whether Vegf signaling also regulates the activity of FGF signaling, we treated embryos with the Vegf inhibitor ZM306416 during somitogenesis. In contrast to the observed epistasis between Wnt16 and FGF signaling in the somites, pharmacological inhibition of Vegf signaling produced no alteration in expression of either pea3 or fgfr4 in the somites compared to DMSO-treated controls (Supplementary Fig. 5c, d). Taken together, these results suggest that Wnt16 regulates the FGF signaling pathway during somitogenesis to specify HSCs.

Somitic expression of *dlc* but not *dld* requires FGF signaling

Previous studies suggest that FGF signaling can control Notch ligand expression in the somites through regulation of the transcription factor FoxD5[41]. Our previous work showed

that Wnt16 is required for *dlc* and *dld* expression[28], but how this regulation is mediated is unknown. Our results above indicate that Wnt16 acts upstream of FGF signaling in HSC specification, suggesting the possibility that FGF signaling might be required for *dlc* and *dld* expression. We therefore tested whether FGF signaling might regulate somitic expression of *dlc* and/or *dld*. To investigate this question, we blocked FGF signaling with a 12 hpf induction of *hsp70:dn-fgfr1* transgenic animals followed by WISH for *dlc* and *dld* at 15 hpf. Loss of FGF signaling led to a loss of somitic *dlc* expression at 15 hpf (Fig. 5a, b). Likewise, the sclerotome marker *foxc1b*, which requires somitic Dlc[28], was reduced in the absence of FGF signaling (Supplementary Fig. 6a). This effect was specific to the somites, since expression of other Notch ligands and receptors, including *dlc* in endothelium at 26 hpf, was not altered (Supplementary Fig. 6b). In addition, pharmacological inhibition using the FGFR antagonist SU5402 led to a robust reduction of *dlc* expression when compared to DMSO-treated controls, whereas ectopic activation of FGF signaling enhanced *dlc* expression in the somites (Fig. 5c, d; Supplementary Fig. 6c). In contrast to the effects of *dlc*, somitic expression of *dld* was not altered following loss of FGF signaling (Fig. 5e–h), indicating that FGF is dispensable for *dld* expression but required specifically for somitic *dlc* expression.

Combined expression of *dlc* and *dld* is required for HSC specification downstream of Wnt16, whereas single knockdown of either ligand incompletely blocked HSC formation[28]. We therefore reasoned that the incomplete loss of HSCs following loss of FGF signaling (Fig. 1e) may be due to residual somitic Notch signaling mediated by *dld.* We therefore tested whether or not combined loss of Dld and FGF function would lead to a more complete loss of HSCs. We analyzed the expression of *runx1* (26 hpf) and *cmyb* (32 hpf) in dld-MO injected *hsp70:dn-fgfr1* and wt control embryos heat-shocked at 12 hpf (Fig. 5i–p). Whereas injection of individual dld-MO into wt embryos led to a loss of *runx1* and *cmyb* expression at levels comparable to heat-induced *hsp70:dn-fgfr1* alone, combinatorial ablation of FGF signaling and Dld function led to significantly lower numbers of HSCs (Fig. 5q, r).

Finally, in order to confirm that FGF signaling acts upstream of *dlc* to specify HSCs, we performed rescue experiments in which *hsp70:dn-fgfr1* animals were injected with *dlc* mRNA at the 1–2-cell stage of development followed by heat-shock at 12 hpf. As assessed by *runx1* and *cmyb* expression, HSC numbers were significantly rescued following injection of *dlc* in the absence of FGF signaling (Fig. 6a–f; Supplementary Fig. 7a). To examine this in another way, we performed rescue experiments with transgenic animals whereby Notch signaling can be experimentally activated by heat-induction (*hsp70:gal4; UAS:NICD-myc*)[14,42]. To obtain triple transgenic animals, hsp70:dn-fgfr1 animals were crossed with hsp70:gal4; UAS:NICD-myc fish. Both dn-Fgfr1 and NICD-myc, transgenes were induced by heat-shock at 12 hpf, and NICD+ transgenic fish were identified by myc-antibody staining after runx1 WISH was performed (Supplementary Fig. 7c). NICD overexpression in hsp70:dn-fgfr1 embryos led to a mild recovery of runx1 expression (Supplementary Fig. 7b, d). Since heat-shock at later timepoints (15 hpf) showed no loss of HSCs in hsp70:dn-fgfr1 embryos (Fig. 1e, f), we performed a second heat shock in triple transgenic embryos to maximize the effects of NICD on HSC specification. A first heat-shock was administered at 12 hpf to ablate FGF signaling by 15 hpf. Next, a second heat-induction was performed at

14 hpf, as this timepoint was previously utilized to optimally rescue HSC specification in wnt16 morphants via NICD induction[28]. WISH for *runx1* at 26 hpf demonstrated that activation of Notch signaling almost fully recovered runx1+ HSCs following ablation of FGF signaling (Fig. 6g–m). Taken together, these results demonstrate that FGF signaling is required for *dlc* but not *dld* expression in somites to regulate HSC specification during somitogenesis.

Fgfr4 acts to relay Wnt16 signals to Dlc to specify HSCs

During early to mid-somitogenesis, knockdown of Wnt16 led to diminished expression of *fgfr4* but no alteration of *fgfr1* in somites (Fig. 4h, i; Supplementary Fig. 5a). Moreover, two-color FISH demonstrated that *dlc* was expressed in *fgfr4*$^+$ but not in *fgfr1*$^+$ somitic tissues (Fig. 7a–f). Based on these results, we hypothesized that Fgfr4 may mediate the Wnt16/Dlc signaling cascade to regulate HSC specification. To test this hypothesis, we knocked down the function of *fgfr4* using both splicing-blocking (Fgfr4-MO1) and translation-blocking (Fgfr4-MO2) receptor-specific MOs. We observed that *dlc* expression in somites at 15 hpf as well as *foxc1b* expression in the sclerotome was reduced in both *fgfr4* morphants when compared to uninjected and control MO injected embryos (Fig. 7g–i; Supplementary Fig. 4a, 8b, c). By contrast, knockdown of *fgfr1* led to no alteration in *dlc* expression (Supplementary Fig. 8a). Finally, to determine if regulation of *dlc* via Fgfr4 is upstream of HSC generation, we analyzed HSC marker expression in *fgfr4* morphants. Loss of Fgfr4 function led to a marked decrease in the number of *runx1*$^+$ and *cmyb*$^+$ cells along the DA (Fig. 7j–o; Supplementary Fig. 7b, c). Although *fgfr4* morphant animals showed slight patterning defects potentially caused by the ablation of *fgfr4* at earlier developmental stages[43], both endothelium and DA appeared normal in the morphants (Fig. 7p–u; Supplementary Fig. 7b). Additionally, knock down of fgfr4 using fgfr4-MO2 led to no alterations in shh and vegf expression, whereas expression of the sclerotomal marker foxc1b was severely reduced (Supplementary Fig. 8d), consistent with our findings in hsp70:dn-fgfr1 transgenic animals (Fig. 2e, f; Supplementary Fig. 2g, 6a). Further analysis of HSC emergence using *cmyb:GFP; kdrl:RFP* transgenic animals[5] showed a marked reduction in the number of *cmyb*$^+$ *kdrl*$^+$ double positive HSCs in *fgfr4* morphants compared to controls (Fig. 7v–y). Taken together, these results indicate that Fgfr4 plays a pivotal role in mediating the Wnt16/Dlc signaling cascade required for instruction of HSC fate.

DISCUSSION

Although roles for FGF signaling in primitive hematopoiesis have been described[21–23], its potential function in the embryonic development of HSCs has not been addressed. Here, we demonstrate that FGF signaling is required for HSC specification through its actions in neighboring somitic tissues. Our studies suggest that FGF signaling in the somite serves to bridge a signaling cascade between a non-canonical Wnt ligand, Wnt16, and the Notch pathway through its regulation of Dlc (Fig. 8).

Inhibition of FGF signaling using inducible transgenic *hsp70:dn-fgfr1* animals reveals that induction of dn-Fgfr1 at 12 hpf led to significantly fewer specified HSCs. Our strategy for time-specific FGF inhibition allowed us to bypass earlier known requirements for FGF

signaling in mesoderm patterning and primitive hematopoiesis[23,30,44,45], and directly examine the later timepoints proximal to HSC specification. These results define a critical requirement for FGF signaling in HSC specification from 14–17 hpf during somitogenesis, after its role in mesoderm formation and primitive blood cell development has passed. Interestingly, as presented in the companion paper (Pouget et al.), even later modulation of the FGF pathway at 20.5 hpf shows an opposite role for FGF signaling, limiting emergence of HSCs from the aortic floor. Our studies indicate that FGF signaling during somitogenesis mediates Wnt16 activation of Dlc within the somite, while our collaborators demonstrate that FGFs negatively regulate HSC formation by restricting a necessary pro-hematopoietic BMP signal at 20.5 hpf. Together with past work, these results demonstrate that the regulation of HSC formation by FGF signaling is dynamic, with multiple independent roles present in distinct temporal windows.

Sonic Hedgehog (Shh) and Vegf play key roles in patterning the DA and regulating emergence of HSCs. During early zebrafish somitogenesis, Shh activates expression of Vegf which in turn is required for expression of Notch1 in the arterial vasculature[31,46,47]. Notch1 is required cell autonomously in the hemogenic endothelium for HSC specification[15]. Our current studies indicate that Fgf signaling does not interact with this pathway. Expression of *shh*, as well as its targets *ptc1* and *ptc2* were not altered following ablation of FGF signaling. No alteration of *vegfa* was observed in somites of FGF-inhibited embryos, and conversely, the FGF target *pea3* was normal in embryos treated with Vegf inhibitors. Moreover, not only did the vasculature develop morphologically normally, endothelial expression of the Notch ligands *dlc* and *dll4*, as well as the receptors *notch1b* and *notch3*, was normal in the absence of FGF signaling. Our results thus indicate that the requirement for FGF signaling in HSC specification is independent of the Shh and Vegf pathways, but rather operates temporally in parallel.

A growing body of evidence supports the idea that gene expression and patterning within the somites play a critical role in HSC specification, but many details remain mysterious. We previously identified an important role for the non-canonical Wnt ligand, Wnt16 in HSC specification. Loss of Wnt16 led to loss of the two key Notch ligands *dlc* and *dld* in the somite. These in turn regulate HSC specification, but whether or not each acts directly on the hemogenic endothelium remains to be determined.

Multiple lines of evidence supported the idea that the temporal 14–17 hpf requirement observed for FGF signaling in HSC specification is operational within the formed somites. The FGF targets *pea3* and *erm* are expressed in the somites, but not the PLM. So are the key receptors, *fgfr1* and *fgfr4*,. As the FGF signaling requirement we have defined here does not interact with the Shh/Vegf/Notch pathway, we examined the possibility that it interacts with the Wnt16/Dlc/Dld pathway[28], which is also operational within the somites. Knockdown of Wnt16 reduces the expression of *pea3* and *fgfr4*, and this loss of expression could be rescued by enforced activation of FGF signaling, revealing Wnt16 is required to turn on, or potentiate somitic FGF signaling. These results reveal a novel non-canonical Wnt/Fgf signaling axis upstream of HSC specification.

To better locate where FGF signaling acts in the Wnt16/Dlc/Dld/HSC specification pathway, we examined the ability of Fgf to regulate expression of the pivotal somitic Notch ligands *dlc* and *dld*. This possibility seemed plausible, given previous studies that have suggested that somitic Notch ligand expression is regulated by FGF signaling[41]. Interestingly *dlc*, but not *dld* requires FGF signaling downstream of Wnt16. We have determined that the key FGFR in this pathway is Fgfr4. Although both *fgfr1* and *fgfr4* are expressed in the somites, only *fgfr4* expression directly overlaps that of *dlc*, and only knockdown of Fgfr4 has significant effects on *dlc* expression. Our results strongly suggest the possibility that Fgfr4 cell-autonomously regulates expression of Dlc, but we cannot exclude the possibility of paracrine relay signaling within the $Fgfr4^+$ population. Consistent with the notion that Fgfr4 is active within the somites and not in the endothelium, knockdown of Fgfr4 yields changes in somitic but not vascular gene expression, leaving endothelial and arterial markers intact.

Importantly, our results locate a requirement for FGF signaling within a now better-defined somitic Wnt16/FGF/Notch HSC specification pathway. FGF signaling here works to activate expression of *dlc* but not *dld*, which represents a parallel input downstream of Wnt16, but not evidently regulated through FGF. $Runx1^+$ HSCs are partially lost in FGF-inhibited conditions and this loss can be rescued by injection of *dlc* mRNA. Consistent with the bifurcation of the pathways downstream of Wnt16 at the point of FGF signaling, HSCs are partially ablated in the absence of FGF signaling, and fully ablated when *dld* is knocked down in parallel to FGF inhibition.

The identification of Fgfr4 as a receptor specifically required for HSC generation begs the question of which FGF ligands are active in this process. Our results demonstrate that Wnt16 is critical for cellular reception of the FGF signal, by activating expression of *fgfr4*, but do not exclude the possibility that it also activates expression of key ligands and downstream signals transduction factors. The FGF ligands FGF1, FGF8, and FGF17 are expressed in developing somites[48–50]. FGF1 increases the generation of long-term repopulating HSCs *in vitro*[25] and is required for primitive hematopoiesis in zebrafish embryos[48]. FGF8 has a critical role in mesoderm formation and patterning[51,52] and zebrafish studies with *fgf8* mutant animals (*ace*) indicate that FGF8 is required for somitogenesis[49]. Likewise, FGF17 potentially plays a role in somite patterning[50]. However, because each of these ligands also has earlier developmental functions, published loss-of-function studies were limited in determining the role of FGFs during the later developmental stages important for hematopoietic specification. Therefore, inducible genetic tools are necessary to further analyze individual roles of FGF ligands in HSC specification.

Although our studies have precisely defined a specific temporal window of somitic signaling required for HSC specification, the relay factors that signal to the adjacent PLM to specify HSC precursors remain to be defined. Multiple studies have now defined specific genetic perturbations in which both sclerotome and HSC specification are abrogated, suggesting the possibility that HSC specification somehow requires the sclerotome. The sclerotome is the ventromedial compartment of developing somites, which gives rise predominantly to elements of the axial skeleton. Sclerotome has been postulated to also give rise to the vascular smooth muscle cells (VSMCs) that sheath the dorsal aorta53–56, but others have

found a different origin57. Similar to wnt16 morphants, and loss of function in either or both of the Notch ligands Dlc and Dld28, loss of FGF signaling by either global ablation or specific knockdown of Fgfr4 led to loss of sclerotomal tissues, suggesting that the Wnt16-FGF-Notch signaling cascade in the somite directs sclerotome development that may subsequently relay necessary signals from the somites to the PLM. Our recent results suggest that one such relay signal is another iteration of Notch signaling, where Notch ligands presented by the sclerotome make direct contact with the shared vascular precursors of HSCs as they migrate to form the pre-aortic vascular cord58. In addition, subsequent signals may be carried by VSMC precursors derived from the sclerotome1. To further address the role of the sclerotome, more tissue-specific transgenic reagents will be necessary to investigate its function and behavior during HSC development.

A second population of somite-derived cells has recently been described that has been suggested to be required for HSC specification, the “endotome”, a *pax3*$^{+}$ population near the septa (vertical somite boundaries), which incorporates into the maturing endothelium[59]. A similar population has previously been described in chick[60] and possibly mouse[54], but was not previously implicated in HSC specification. The Wnt16/FGF/Notch pathway appears to be discrete from the endotomal pathway, most notably in that the affected regions of the somite are different (*foxc1b*$^{+}$ sclerotome versus *pax3*$^{+}$ septa), but we cannot rule out the possibility that Wnt16/FGF/Notch regulates both endotomal and sclerotomal contributions to HSC specification. The fact that in *choker* mutants—which display an increased contribution of somite-derived cells to the endothelium of the dorsal aorta–*wnt16* expression is nearly ablated suggests that the *choker* mutation (*meox1a*) short circuits the requirement for Wnt16[59], for example by leading to an upregulation of FGF signaling or enhanced presentation of Notch ligands.

In conclusion, our studies suggest that FGF signaling through Fgfr4 is required to mediate a signaling cascade between Wnt16 and Dlc in the developing somite to specify HSCs. These findings provide a better understanding of HSC ontogeny and have elucidated a novel set of regulatory inputs necessary for HSC development. Importantly, our findings shed light on pathways that can be potentially modulated to instruct *in vitro* production of HSCs from pluripotent precursors, a process that has proven to be extremely challenging.

METHODS

Zebrafish husbandry

Wild-type AB* and transgenic *hsp70:dn-fgfr1* (Tg(*hsp70l:dnfgfr1-EGFP*)^{pd1})[27], Tg(*cmyb:EGFP*)^{zf169} [61], Tg(*kdrl:RFP*)^{la4} [62], *hsp70:ca-fgfr1* (Tg(*hsp70l:Xla.fgfr1, cryaa:DsRed*)^{pd3})[40], *UAS:NICD-myc* (Tg(*5xUAE-E1b:6xMYC-notch1a*)^{kca3})[42], *hsp70:gal4* (Tg(*−1.5hsp70l:Gal4*)^{kca4})[42], *fli1:EGFP* (Tg(*fli1a:EGFP*)^{y1})[63], *α-actin:GFP* (Tg(*actc1b:GFP*)^{zf13})[64] zebrafish embryos and adult fish were raised in a circulating aquarium system (Aquaneering) at 28°C and maintained in accordance with UCSD Institutional Animal Care and Use Committee (IACUC) guidelines. For heat-shocking transgenic embryos, *hsp70:dn-fgfr1* and *hsp70:ca-fgfr1* embryos were placed in E3 fish water in a 125 ml flask and transferred to a 38°C water bath for 20 min or 45 min at 12, 15, or 17 hpf. For double heat-shock of *hsp70:gal4; UAS:myc-Notch1a-intra; hsp70:dn-fgfr1*

transgenics, embryos in E3 water in a 125 ml flask were incubated in a 38°C water bath for 20 min at 12 hpf, followed by a 45 min incubation in a 38°C water bath at 15 hpf.

WISH

Whole-mount single or double enzymatic in situ hybridization was performed on embryos fixed overnight with 4% paraformaldehyde (PFA) in phosphate buffered saline (PBS). Fixed embryos were washed briefly in PBS and transferred stepwise into methanol in PBS for storage at −20°C. Embryos were rehydrated stepwise through methanol in PBS–0.1% Tween 20 (PBT). Rehydrated embryo samples were then incubated with 10 μg/ml proteinase K in PBT for 5 min for 5 to 10 somite stage (12 – 15 hpf) embryos and 15 min for 24 to 36 hpf embryos. After proteinase K treatment, samples were washed in PBT and refixed in 4% PFA for 20 min at room temperature. After washes in two changes of PBT, embryos were prehybridized at 65°C for 1 hour in hybridization buffer (50% formamide, 5x SSC, 500 μg/mL torula (yeast) tRNA, 50 μg/mL heparin, 0.1% Tween 20, 9 mM citric acid (pH 6.5)). Samples were then hybridized overnight in hybridization buffer including digoxigenin- (DIG) or fluorescein- labeled RNA probe. After hybridization, experimental samples were washed stepwise at 65°C for 15 min each in hybridization buffer in 2x SSC mix (75%, 50%, 25%), followed by two washes with 0.2x SSC for 30 min each at 65°C. Further washes were performed at room temperature for 5 min each with 0.2x SSC in PBT (75%, 50%, 25%). Samples were incubated in PBT with 2% heat-inactivated goat serum and 2 mg/ml bovine serum albumin (block solution) for 1 hour and then incubated overnight at 4°C in block solution with diluted DIG-antibodies (1:5000) conjugated with alkaline phosphatase (AP) (Roche). To visualize WISH signal, samples were washed three times in AP reaction buffer (100mM Tris, pH 9.5, 50 mM $MgCl_2$, 100mM NaCl, 0.1% Tween 20, 1mM levamisole (Sigma)) for 5 min each and then incubated in the AP reaction buffer with NBT/BCIP substrate (Promega).

For double enzymatic WISH, the processed samples were washed in 0.1M glycine (pH 2.2) for 20 min and then washed in PBT for 5 min. After storing washed samples in methanol for 1 hour, the embryos samples were stepwise rehydrated in methanol in PBT for 5 min each (75%, 50%, 25%) and further washed in PBT. After incubation in block solution for 1 hour, the samples were incubated overnight at 4°C in block solution with diluted fluorescein-antibodies (1:5000) conjugated with AP (Roche). After PBT washes, the samples were washed two times in 0.1M Tris-HCl (pH 8.2). Embryos were then incubated in 0.1M Tris-HCl (pH 8.2) with Fast Red Tablets (Roche). After obtaining red signals, embryos were washed in in 0.1M Tris-HCl (pH 8.2) and refixed in 4% PFA.

For two-color double FISH, embryos were blocked in maleic acid buffer (MAB; 150 mM maleic acid, 100 mM NaCl, pH 7.5) with 2% Roche Blocking Reagent (MABB) for 1 hour at room temperature, after hybridizing at 65°C with probes as described above. Embryos were incubated overnight at 4°C in MABB with anti-fluorescein POD (Roche) at a 1:500 dilution. After four washes in MAB for 20 min each followed by washes in PBS at room temperature, embryo samples were incubated in TSA Plus Fluorescein Solution (Perkin Elmer) for 1 hour. Embryos were washed 10 min each in methanol in PBS (25%, 50%, 75%, 100%). Embryos were incubated in 1% H_2O_2 in methanol for 30 min at room temperature

and washed for 10 min each in methanol in PBS (75%, 50% 25%) and 10 min in PBS. After blocking for 1 hour in MABB, embryos were incubated overnight at 4°C in MABB with anti-DIG POD (Roche) at a 1:1000 dilution. Samples were washed and incubated in TSA Plus CY3 solution (Perkin Elmer) as described above. Embryos were washed three times for 10 min each in PBT and refixed in 4% PFA after the staining was complete.

Antisense RNA probes for the following genes were prepared using probes containing DIG or fluorescein labeled UTP: *runx1*, *cmyb*, *rag1*, *pea3*, er*m*, *scl*, *lmo2*, *cdx4*, *shh*, *desma*, *kdrl*, *cdh5*, *gata1*, *l-plastin*, *efnb2a*, *fli1*, *fgfr1*, *fgfr2*, *fgfr3*, *fgfr4*, *dlc*, *dld*, *dll4*, *notch1b*, *notch3*, *wnt16*, *foxc1b*.

Immunofluorescence and microscopy

For immunofluorescence staining for Myc in *hsp70:gal4; UAS:NICD-myc* zebrafish embryos after WISH, 100% acetone was added to the embryos (7min at −20°C) instead of proteinase K during the WISH procedure described above. WISH samples of embryos were blocked in MABB for 1 hour and incubated overnight in MABB with anti-Myc monoclonal 9E10 antibodies at 1:100 (Covance). After four washes in MABB for 30 min each, embryos were incubated in Dylight 488 AffiniPure donkey anti-mouse IgG secondary antibodies (Jackson Immunoresearch Laboratories) at 1:100 in MABB. After staining, embryos were washed in MABB for four times for 30 min each. The samples were imaged using a stereo zoom microscope (Zeiss, Axio Zoom). Live *hsp70:dn-fgfr1* and *kdrl:RFP; cmyb:EGFP* transgenic embryos and flat-mount or whole-mount two-color double FISH samples were imaged using confocal microscopy (Leica, SP5). GFP and fluorescein were excited by a 488 nm laser, while DsRed and CY3 were excited by 543 nm.

Pharmacological treatment

SU5402 (Calbiochem) and ZM306416 (Tocris) was dissolved in DMSO at a concentration of 10mM. Zebrafish AB* embryos were incubated in 5 ml of 5 μM SU5402 solution from 12 – 15 hpf and 5 μM ZM306416 solution from 10 hpf in the dark, followed by fixation with 4% PFA.

Microinjections of morpholinos and mRNA

Antisense morpholinos (MOs; Gene Tools, LLC) were diluted as 1mM or 3mM stock in DEPC-treated H_2O. 5ng of standard control MO (St.CoMO)[65], wnt16-MO[28], dld-MO2[28], fgfr1-MO1[66], fgfr4-MO1[67], fgfr4-CoMO2 and fgfr4-MO2 were injected at the 1- to 2-cell stage of development. The sequence of translation-blocking targeted fgfr4-MO2 is 5′-AGATGCTCAACATCTTGCTGAGGTA-3′ and 5 base pair mismatched fgfr4 control MO2 (fgfr4-CoMO2) is 5′-AaATGaTCAAaATCTTaCTGAaGTA-3′ (lower case letter indicates mismatched base pairs). Full-length *dlc* mRNA was synthesized from linearized pCS2+ *dlc*[28] with the mMessega mMaching kit (Ambion). *dlc* mRNA was injected with 100pg into 1- to 2-cell stage *hsp70:dn-fgfr1* transgenic embryos for rescue experiments. All microinjections were performed with the indicated concentration of RNA or MO in a volume of 1nl using a PM 1000 cell microinjector (MDI).

FACS

fli1:EGFP and *α-actin:GFP* embryos (~50 embryos each) at 17 hpf were dissociated in PBS by homogenizing with sterile plastic pestle or pipette. Dissociated cells were filtered through 40μm nylon cell strainer (Falcon 2340) and then rinsed with PBS with 1% fetal bovine serum. Propidium iodide (Sigma) was added (1μg/ml) to exclude dead cells and debris. FACS was performed based on GFP fluorescence[5] with a FACS Aria II flow cytometer (Beckton Dickinson).

Quantitative real-time PCR

Total RNA was collected from posterior trunk of the embryos or whole embryos (~30 embryos) using TRIzol reagent (Ambion, Life Technologies) and isolated *fli1:EGFP*$^+$ and *α-actin:GFP*$^+$ cells with the RNeasy kit (Qiagen). cDNA was generated from total RNA with iScript cDNA synthesis kit (Bio Rad). The following primers were used for cDNA quantification: *ef1α* (forward, 5′-GAGAAGTTCGAGAAGGAAGC-3′; reverse, 5′-CGTAGTATTTGCTGGTCTCG-3′)[33], *runx1* (forward, 5′-CGGTGAACGGTTAATATGAC-3′; reverse, 5′-CTTTTCATCACGGTTTATGC-3′)[33], *kdrl (*forward, *5′*-CTCCTGTACAGCAAGGAATG-3′; reverse, 5′-ATCTTTGGGCACCTTATAGC-3′)[5], *erm (*forward, 5′-GGTGCCTCCAAATAAGTCTC-3′, reverse 5′-TGGAAATCTGGAACAAACTG-3′), *efnb2a* (forward, 5′-CCCATTTCCCCCAAAGACTA-3′; reverse, 5′-CTTCCCCATGAGGAGATGC-3′), *fgfr1* (forward, 5′-AGTGATGTGGAGTTCGAGTG-3′; reverse, 5′-CAAGCAGGTGTACTCTCCAG-3′) and *fgfr4* (forward, 5′-CAAACAACTTGTGGAAGAGC-3′; reverse, 5′-AGCATCATGGGTAAACACAG-3′).

Supplementary Material

Refer to Web version on PubMed Central for supplementary material.

Acknowledgments

We thank K.D. Poss for sharing transgenic animals and in situ probes, D. Yelon for sharing imaging equipment, and K. Ong and R. Rainville for animal care. Y.L. was supported by a postdoctoral fellowship from the American Heart Association. This work was supported by Innovative Science Award #12PILT12860010 from the American Heart Association, R01-DK074482 and R01-HL119056 from the National Institutes of Health (D.T.).

References

1. Clements WK, Traver D. Signalling pathways that control vertebrate haematopoietic stem cell specification. Nature reviews Immunology. 2013; 13:336–348.10.1038/nri3443
2. McGrath KE, Palis J. Hematopoiesis in the yolk sac: more than meets the eye. Experimental hematology. 2005; 33:1021–1028.10.1016/j.exphem.2005.06.012 [PubMed: 16140150]
3. Medvinsky AL, Dzierzak EA. Development of the definitive hematopoietic hierarchy in the mouse. Developmental and comparative immunology. 1998; 22:289–301. [PubMed: 9700459]
4. Cumano A, Godin I. Ontogeny of the hematopoietic system. Annual review of immunology. 2007; 25:745–785.10.1146/annurev.immunol.25.022106.141538
5. Bertrand JY, et al. Haematopoietic stem cells derive directly from aortic endothelium during development. Nature. 2010; 464:108–111.10.1038/nature08738 [PubMed: 20154733]

6. Peeters M, et al. Ventral embryonic tissues and Hedgehog proteins induce early AGM hematopoietic stem cell development. Development. 2009; 136:2613–2621.10.1242/dev.034728 [PubMed: 19570846]
7. Dyer MA, Farrington SM, Mohn D, Munday JR, Baron MH. Indian hedgehog activates hematopoiesis and vasculogenesis and can respecify prospective neurectodermal cell fate in the mouse embryo. Development. 2001; 128:1717–1730. [PubMed: 11311154]
8. Gering M, Patient R. Hedgehog signaling is required for adult blood stem cell formation in zebrafish embryos. Developmental cell. 2005; 8:389–400.10.1016/j.devcel.2005.01.010 [PubMed: 15737934]
9. Cleaver O, Krieg PA. VEGF mediates angioblast migration during development of the dorsal aorta in Xenopus. Development. 1998; 125:3905–3914. [PubMed: 9729498]
10. Leung A, et al. Uncoupling VEGFA functions in arteriogenesis and hematopoietic stem cell specification. Developmental cell. 2013; 24:144–158.10.1016/j.devcel.2012.12.004 [PubMed: 23318133]
11. Shalaby F, et al. A requirement for Flk1 in primitive and definitive hematopoiesis and vasculogenesis. Cell. 1997; 89:981–990. [PubMed: 9200616]
12. Gupta S, Zhu H, Zon LI, Evans T. BMP signaling restricts hemato-vascular development from lateral mesoderm during somitogenesis. Development. 2006; 133:2177–2187.10.1242/dev.02386 [PubMed: 16672337]
13. Maeno M, et al. The role of BMP-4 and GATA-2 in the induction and differentiation of hematopoietic mesoderm in Xenopus laevis. Blood. 1996; 88:1965–1972. [PubMed: 8822915]
14. Burns CE, Traver D, Mayhall E, Shepard JL, Zon LI. Hematopoietic stem cell fate is established by the Notch-Runx pathway. Genes & development. 2005; 19:2331–2342.10.1101/gad.1337005 [PubMed: 16166372]
15. Hadland BK, et al. A requirement for Notch1 distinguishes 2 phases of definitive hematopoiesis during development. Blood. 2004; 104:3097–3105.10.1182/blood-2004-03-1224 [PubMed: 15251982]
16. Kumano K, et al. Notch1 but not Notch2 is essential for generating hematopoietic stem cells from endothelial cells. Immunity. 2003; 18:699–711. [PubMed: 12753746]
17. Aulehla A, Pourquie O. Signaling gradients during paraxial mesoderm development. Cold Spring Harbor perspectives in biology. 2010; 2:a000869.10.1101/cshperspect.a000869 [PubMed: 20182616]
18. Schier AF, Talbot WS. Molecular genetics of axis formation in zebrafish. Annual review of genetics. 2005; 39:561–613.10.1146/annurev.genet.37.110801.143752
19. Murakami M, Simons M. Fibroblast growth factor regulation of neovascularization. Current opinion in hematology. 2008; 15:215–220.10.1097/MOH.0b013e3282f97d98 [PubMed: 18391788]
20. Presta M, et al. Fibroblast growth factor/fibroblast growth factor receptor system in angiogenesis. Cytokine & growth factor reviews. 2005; 16:159–178.10.1016/j.cytogfr.2005.01.004 [PubMed: 15863032]
21. Walmsley M, Cleaver D, Patient R. Fibroblast growth factor controls the timing of Scl, Lmo2, and Runx1 expression during embryonic blood development. Blood. 2008; 111:1157–1166.10.1182/blood-2007-03-081323 [PubMed: 17942750]
22. Nakazawa F, Nagai H, Shin M, Sheng G. Negative regulation of primitive hematopoiesis by the FGF signaling pathway. Blood. 2006; 108:3335–3343.10.1182/blood-2006-05-021386 [PubMed: 16888091]
23. Yamauchi H, et al. Fgf21 is essential for haematopoiesis in zebrafish. EMBO reports. 2006; 7:649–654.10.1038/sj.embor.7400685 [PubMed: 16612391]
24. Berardi AC, Wang A, Abraham J, Scadden DT. Basic fibroblast growth factor mediates its effects on committed myeloid progenitors by direct action and has no effect on hematopoietic stem cells. Blood. 1995; 86:2123–2129. [PubMed: 7662960]
25. de Haan G, et al. In vitro generation of long-term repopulating hematopoietic stem cells by fibroblast growth factor-1. Developmental cell. 2003; 4:241–251. [PubMed: 12586067]
26. Zhao M, et al. FGF signaling facilitates postinjury recovery of mouse hematopoietic system. Blood. 2012; 120:1831–1842.10.1182/blood-2011-11-393991 [PubMed: 22802336]

27. Lee Y, Grill S, Sanchez A, Murphy-Ryan M, Poss KD. Fgf signaling instructs position-dependent growth rate during zebrafish fin regeneration. Development. 2005; 132:5173–5183.10.1242/dev.02101 [PubMed: 16251209]
28. Clements WK, et al. A somitic Wnt16/Notch pathway specifies haematopoietic stem cells. Nature. 2011; 474:220–224.10.1038/nature10107 [PubMed: 21654806]
29. Dequeant ML, et al. A complex oscillating network of signaling genes underlies the mouse segmentation clock. Science. 2006; 314:1595–1598.10.1126/science.1133141 [PubMed: 17095659]
30. Yamaguchi TP, Harpal K, Henkemeyer M, Rossant J. fgfr-1 is required for embryonic growth and mesodermal patterning during mouse gastrulation. Genes & development. 1994; 8:3032–3044. [PubMed: 8001822]
31. Gering M, Patient R. Notch signalling and haematopoietic stem cell formation during embryogenesis. Journal of cellular physiology. 2010; 222:11–16.10.1002/jcp.21905 [PubMed: 19725072]
32. Kissa K, Herbomel P. Blood stem cells emerge from aortic endothelium by a novel type of cell transition. Nature. 2010; 464:112–115.10.1038/nature08761 [PubMed: 20154732]
33. Bertrand JY, Kim AD, Teng S, Traver D. CD41+ cmyb+ precursors colonize the zebrafish pronephros by a novel migration route to initiate adult hematopoiesis. Development. 2008; 135:1853–1862.10.1242/dev.015297 [PubMed: 18417622]
34. Munchberg SR, Ober EA, Steinbeisser H. Expression of the Ets transcription factors erm and pea3 in early zebrafish development. Mechanisms of development. 1999; 88:233–236. [PubMed: 10534622]
35. Roehl H, Nusslein-Volhard C. Zebrafish pea3 and erm are general targets of FGF8 signaling. Current biology : CB. 2001; 11:503–507. [PubMed: 11413000]
36. Patterson LJ, et al. The transcription factors Scl and Lmo2 act together during development of the hemangioblast in zebrafish. Blood. 2007; 109:2389–2398.10.1182/blood-2006-02-003087 [PubMed: 17090656]
37. Ren X, Gomez GA, Zhang B, Lin S. Scl isoforms act downstream of etsrp to specify angioblasts and definitive hematopoietic stem cells. Blood. 2010; 115:5338–5346.10.1182/blood-2009-09-244640 [PubMed: 20185582]
38. Zhong TP, Childs S, Leu JP, Fishman MC. Gridlock signalling pathway fashions the first embryonic artery. Nature. 2001; 414:216–220.10.1038/35102599 [PubMed: 11700560]
39. Goldfarb M. Signaling by fibroblast growth factors: the inside story. Science's STKE : signal transduction knowledge environment. 2001; 2001:pe37.10.1126/stke.2001.106.pe37
40. Marques SR, Lee Y, Poss KD, Yelon D. Reiterative roles for FGF signaling in the establishment of size and proportion of the zebrafish heart. Developmental biology. 2008; 321:397–406.10.1016/j.ydbio.2008.06.033 [PubMed: 18639539]
41. Lee HC, Tseng WA, Lo FY, Liu TM, Tsai HJ. FoxD5 mediates anterior-posterior polarity through upstream modulator Fgf signaling during zebrafish somitogenesis. Developmental biology. 2009; 336:232–245.10.1016/j.ydbio.2009.10.001 [PubMed: 19818746]
42. Scheer N, Campos-Ortega JA. Use of the Gal4-UAS technique for targeted gene expression in the zebrafish. Mechanisms of development. 1999; 80:153–158. [PubMed: 10072782]
43. Thisse B, Thisse C, Weston JA. Novel FGF receptor (Z-FGFR4) is dynamically expressed in mesoderm and neurectoderm during early zebrafish embryogenesis. Developmental dynamics : an official publication of the American Association of Anatomists. 1995; 203:377–391.10.1002/aja.1002030309 [PubMed: 8589434]
44. Amaya E, Musci TJ, Kirschner MW. Expression of a dominant negative mutant of the FGF receptor disrupts mesoderm formation in Xenopus embryos. Cell. 1991; 66:257–270. [PubMed: 1649700]
45. Griffin K, Patient R, Holder N. Analysis of FGF function in normal and no tail zebrafish embryos reveals separate mechanisms for formation of the trunk and the tail. Development. 1995; 121:2983–2994. [PubMed: 7555724]

46. Lawson ND, Vogel AM, Weinstein BM. sonic hedgehog and vascular endothelial growth factor act upstream of the Notch pathway during arterial endothelial differentiation. Developmental cell. 2002; 3:127–136. [PubMed: 12110173]
47. Rowlinson JM, Gering M. Hey 2 acts upstream of Notch in hematopoietic stem cell specification in zebrafish embryos. Blood. 2010; 116:2046–2056.10.1182/blood-2009-11-252635 [PubMed: 20511544]
48. Songhet P, Adzic D, Reibe S, Rohr KB. fgf1 is required for normal differentiation of erythrocytes in zebrafish primitive hematopoiesis. Developmental dynamics : an official publication of the American Association of Anatomists. 2007; 236:633–643.10.1002/dvdy.21056 [PubMed: 17219402]
49. Reifers F, et al. Fgf8 is mutated in zebrafish acerebellar (ace) mutants and is required for maintenance of midbrain-hindbrain boundary development and somitogenesis. Development. 1998; 125:2381–2395. [PubMed: 9609821]
50. Cao Y, et al. fgf17b, a novel member of Fgf family, helps patterning zebrafish embryos. Developmental biology. 2004; 271:130–143.10.1016/j.ydbio.2004.03.032 [PubMed: 15196956]
51. Draper BW, Stock DW, Kimmel CB. Zebrafish fgf24 functions with fgf8 to promote posterior mesodermal development. Development. 2003; 130:4639–4654.10.1242/dev.00671 [PubMed: 12925590]
52. Pourquie O. Vertebrate segmentation: from cyclic gene networks to scoliosis. Cell. 2011; 145:650–663.10.1016/j.cell.2011.05.011 [PubMed: 21620133]
53. Pouget C, Pottin K, Jaffredo T. Sclerotomal origin of vascular smooth muscle cells and pericytes in the embryo. Developmental biology. 2008; 315:437–447.10.1016/j.ydbio.2007.12.045 [PubMed: 18255054]
54. Wasteson P, et al. Developmental origin of smooth muscle cells in the descending aorta in mice. Development. 2008; 135:1823–1832.10.1242/dev.020958 [PubMed: 18417617]
55. Wiegreffe C, Christ B, Huang R, Scaal M. Sclerotomal origin of smooth muscle cells in the wall of the avian dorsal aorta. Developmental dynamics : an official publication of the American Association of Anatomists. 2007; 236:2578–2585.10.1002/dvdy.21279 [PubMed: 17685486]
56. Wiegreffe C, Christ B, Huang R, Scaal M. Remodeling of aortic smooth muscle during avian embryonic development. Developmental dynamics : an official publication of the American Association of Anatomists. 2009; 238:624–631.10.1002/dvdy.21888 [PubMed: 19235723]
57. Esner M, et al. Smooth muscle of the dorsal aorta shares a common clonal origin with skeletal muscle of the myotome. Development. 2006; 133:737–749.10.1242/dev.02226 [PubMed: 16436625]
58. Kobayashi I, et al. Jam1a-Jam2a interactions regulate haematopoietic stem cell fate through Notch signalling. Nature. 2014; 512:319–323.10.1038/nature13623 [PubMed: 25119047]
59. Nguyen PD, et al. Haematopoietic stem cell induction by somite-derived endothelial cells controlled by meox1. Nature. 2014; 512:314–318.10.1038/nature13678 [PubMed: 25119043]
60. Pouget C, Gautier R, Teillet MA, Jaffredo T. Somite-derived cells replace ventral aortic hemangioblasts and provide aortic smooth muscle cells of the trunk. Development. 2006; 133:1013–1022.10.1242/dev.02269 [PubMed: 16467362]
61. North TE, et al. Prostaglandin E2 regulates vertebrate haematopoietic stem cell homeostasis. Nature. 2007; 447:1007–1011.10.1038/nature05883 [PubMed: 17581586]
62. Huang H, Zhang B, Hartenstein PA, Chen JN, Lin S. NXT2 is required for embryonic heart development in zebrafish. BMC developmental biology. 2005; 5:7.10.1186/1471-213X-5-7 [PubMed: 15790397]
63. Lawson ND, Weinstein BM. In vivo imaging of embryonic vascular development using transgenic zebrafish. Developmental biology. 2002; 248:307–318. [PubMed: 12167406]
64. Higashijima S, Okamoto H, Ueno N, Hotta Y, Eguchi G. High-frequency generation of transgenic zebrafish which reliably express GFP in whole muscles or the whole body by using promoters of zebrafish origin. Developmental biology. 1997; 192:289–299. [PubMed: 9441668]
65. Stachura DL, et al. The zebrafish granulocyte colony-stimulating factors (Gcsfs): 2 paralogous cytokines and their roles in hematopoietic development and maintenance. Blood. 2013; 122:3918–3928.10.1182/blood-2012-12-475392 [PubMed: 24128862]

66. Scholpp S, Groth C, Lohs C, Lardelli M, Brand M. Zebrafish fgfr1 is a member of the fgf8 synexpression group and is required for fgf8 signalling at the midbrain-hindbrain boundary. Dev Genes Evol. 2004; 214:285–295.10.1007/s00427-004-0409-1 [PubMed: 15221377]

67. Nakayama Y, et al. Fgf19 is required for zebrafish lens and retina development. Developmental biology. 2008; 313:752–766.10.1016/j.ydbio.2007.11.013 [PubMed: 18089288]

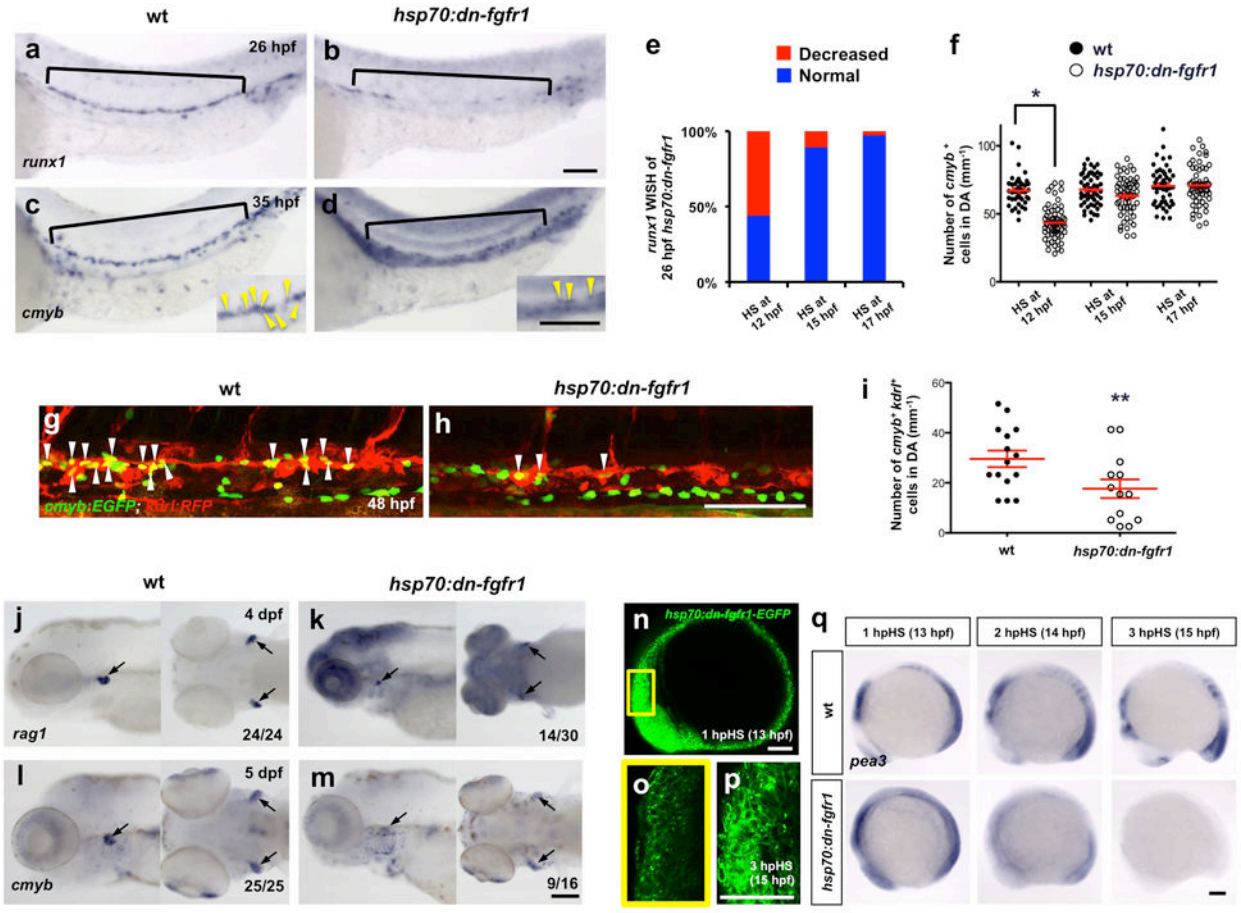

Figure 1. FGF signaling is required for HSC specification during mid-somitogenesis stages

(**a–d**) *hsp70:dn-fgfr1* transgenic embryos, heat-induced at 12 hpf (38°C, 20 min) visualized by WISH for HSC markers *runx1* (black brackets) (**a, b**) and *cmyb* (black brackets and yellow arrowheads in high magnification images) (**c, d**) in aortic hemogenic endothelium compared to wt embryos. (**e**) *runx1* phenotype percentages in *hsp70:dn-fgfr1* animals following heat-shock at the indicated stages (12 hpf, n=82 ; 15 hpf, n=26 ;17 hpf, n=38). (**f**) Quantification of 35 hpf *cmyb*$^{+}$ cells (yellow arrowheads in **c, d**) in the DA of wt and *hsp70:dn-fgfr1* induced at 12 hpf (wt, n=42; *hsp70:dn-fgfr1*, n=61; **P*-value < 0.00001, significantly different from wt, Student's *t*-test), 15 hpf (wt, n=52; *hsp70:dn-fgfr1*, n=56), and 17 hpf (wt, n=48; *hsp70:dn-fgfr1*, n=54). Red lines indicate *mean* ± *s. e. m.* (**g, h**) Confocal microscopy images of 48 hpf Double-positive HSCs (white arrowheads) in *cmyb:EGFP; kdrl;RFP; hsp70:dn-fgfr1* animals following heat-shock at 12 hpf. (**i**) Quantification of 48 hpf *cmyb*$^{+}$ *kdrl*$^{+}$ double positive HSCs in the DA of wt and *hsp70:dn-fgfr1* animals induced at 12 hpf (wt, n=15; *hsp70:dn-fgfr1*, n=13; ***P*-value < 0.005, significantly different from wt, Student's *t*-test). (**j–m**) Lateral and ventral view of WISH images using *hsp70:dn-fgfr1* transgenic embryos heat-induced at 12 hpf for *rag1* at 4dpf (**j, k**) and *cmyb* at 5 dpf (**l, m**) in thymus (black arrows) compared to wt embryos. (**n–p**) Confocal microscopy images of *hsp70:dn-fgfr1* embryos heat-shocked at 12 hpf. Expression of dominant-negative Fgfr1-EGFP at 13 hpf (**n, o**) and 15 hpf (**q**). (**o**) is the magnified region boxed in yellow shown in (**n**). (**q**) WISH for the FGF target *pea3* in wt (top row) and

hsp70:dn-fgfr1 embryos (bottom row) at 13, 14, and 15 hpf after heat-shock at 12 hpf. Scale bars=100μm.

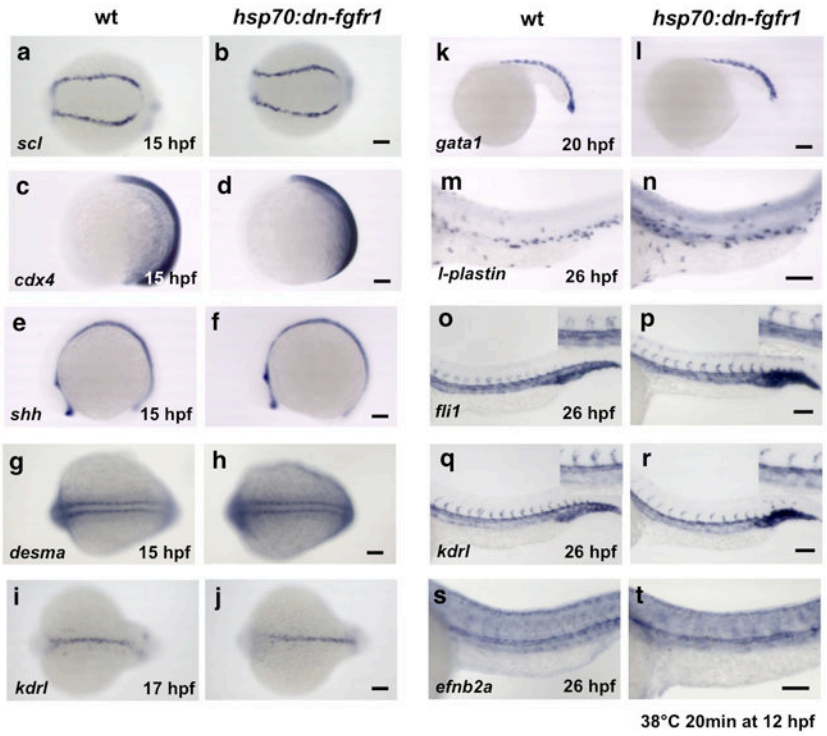

Figure 2. The effect of FGF signaling on HSC formation is specific

WISH of wt and induced *hsp70:dn-fgfr1* at 12 hpf with the PLM markers *scl* (**a, b**) at 15 hpf, the ventral mesoderm marker *cdx4* at 15 hpf (**c, d**), the floorpalte and notochord marker *shh* at 15 hpf (**e, f**) and the somite marker *desma* at 15 hpf (**g, h**), the endothelial marker *kdrl* at 17 hpf (**i, j**), the primitive erythroid marker *gata1* at 20 hpf (**k, l**), the primitive leukocyte marker *l-plastin* at 26 hpf (**m, n**), the endothelial markers *fli1* and *kdrl* at 26 hpf (**o–r**; expression in the aorta and vein with higher magnification included), and the arterial marker *efnb2a* at 26 hpf (**s, t**). Scale bars=100μm.

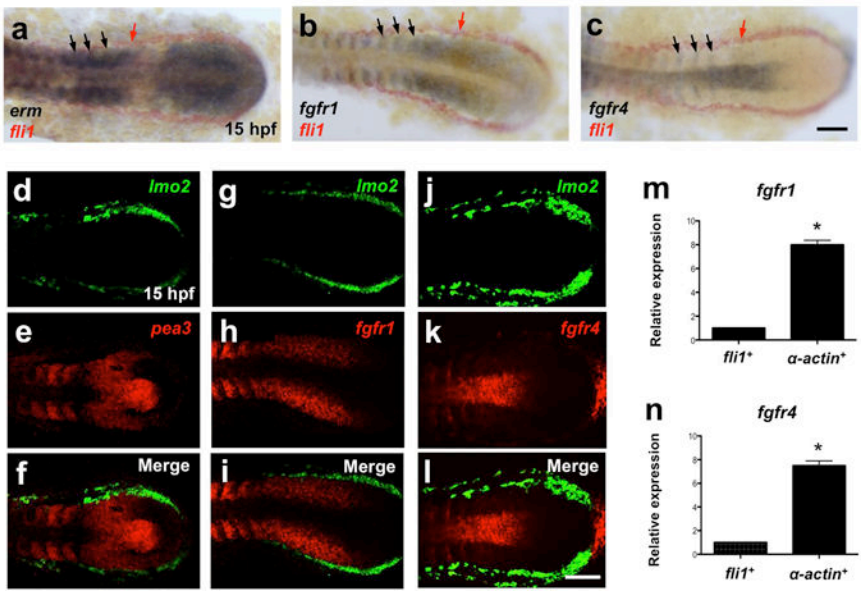

Figure 3. FGF signaling is active in somitic tissues but not in the pre-endothelial PLM during mid-somitogenesis

(**a–c**) Images of double enzymatic WISH using probes for the FGF target gene *erm* (**a**), *fgfr1* (**b**), and *fgfr4* (**c**) expressed in somites (black arrows) and the PLM marker *fli1* (red arrows) at 15 hpf. (**d–l**) Confocal images of two-color FISH with the PLM marker *lmo2* (green in **d, g, j**), *fgfr1, fgfr4* and the FGF target gene *pea3* (red in **e, h, k**) and merged images (**f, i, l**). (**m, n**) qRT-PCR expression of pre-endothelial PLM *fli1:EGFP*$^{+}$ cells and somite-specific *α-actin:GFP*$^{+}$ cells at 17 hpf. Expression data were normalized to *ef1α* levels (*α-actin*$^{+}$ fraction, n=3; **P*-value < 0.005, significantly different from *fli1*$^{+}$, Student's *t*-test). Scale bars=100μm.

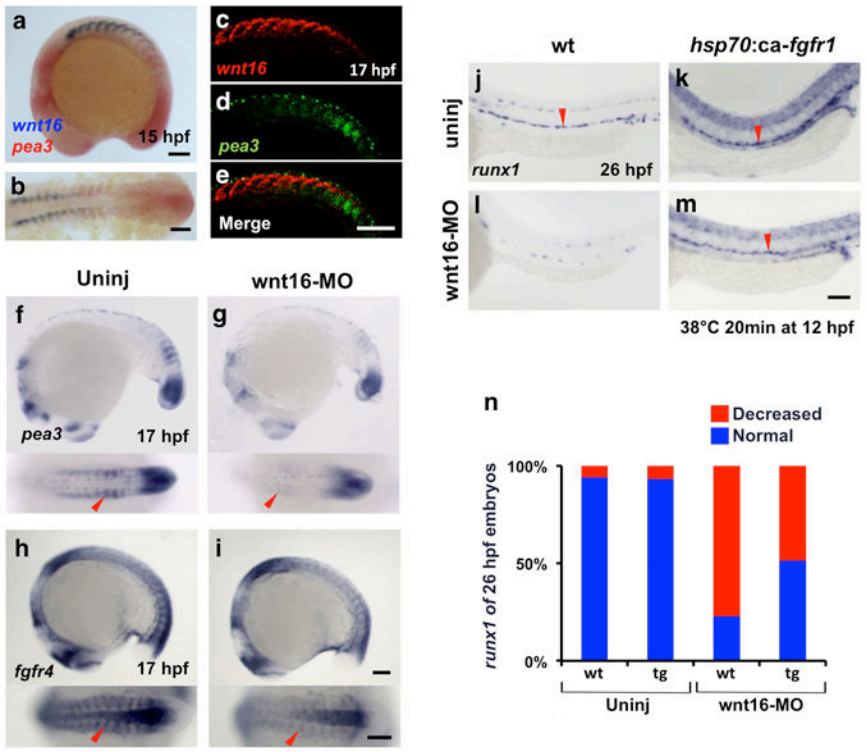

Figure 4. Wnt16 controls FGF signaling activity

(**a, b**) Expression of *wnt16* (blue) and *pea3* (red) at 15 hpf by two-color enzymatic whole-mount and flat-mount in situ hybridization. (**c–e**) Confocal images of FISH for *wnt16* (red in **c**), *pea3* (green in **d**), or merge (**e**) at 17 hpf. (**f–i**) Lateral and dorsal views of expression of *pea3* (**f, g**) and *fgfr4* (**h, i**) in *wnt16* morphants at 17 hpf compared to uninjected controls as indicated at top. (**j–m**) WISH for *runx1* expression (black arrowheads) at 26 hpf following ectopic activation of FGF signaling using *hsp70:ca-fgfr1* induced at 12 hpf (38°C 20 min) in *wnt16* morphants. (**n**) *runx1* phenotype percentages in wnt16-MO injected *hsp70:ca-fgfr1* transgenic embryos (tg) heat-shocked at 12 hpf, compared to wnt16-MO injected wt embryos (uninjected wt, n=34; uninjected tg, n=44; wnt16-MO injected wt, n=48; wnt16-MO injected tg, n=37). Red arrowheads indicate WISH signals of *pea3* and *fgfr4* in the somites (**f–i**) and *runx1* in the DA (**j–m**). Scale bars=100μm.

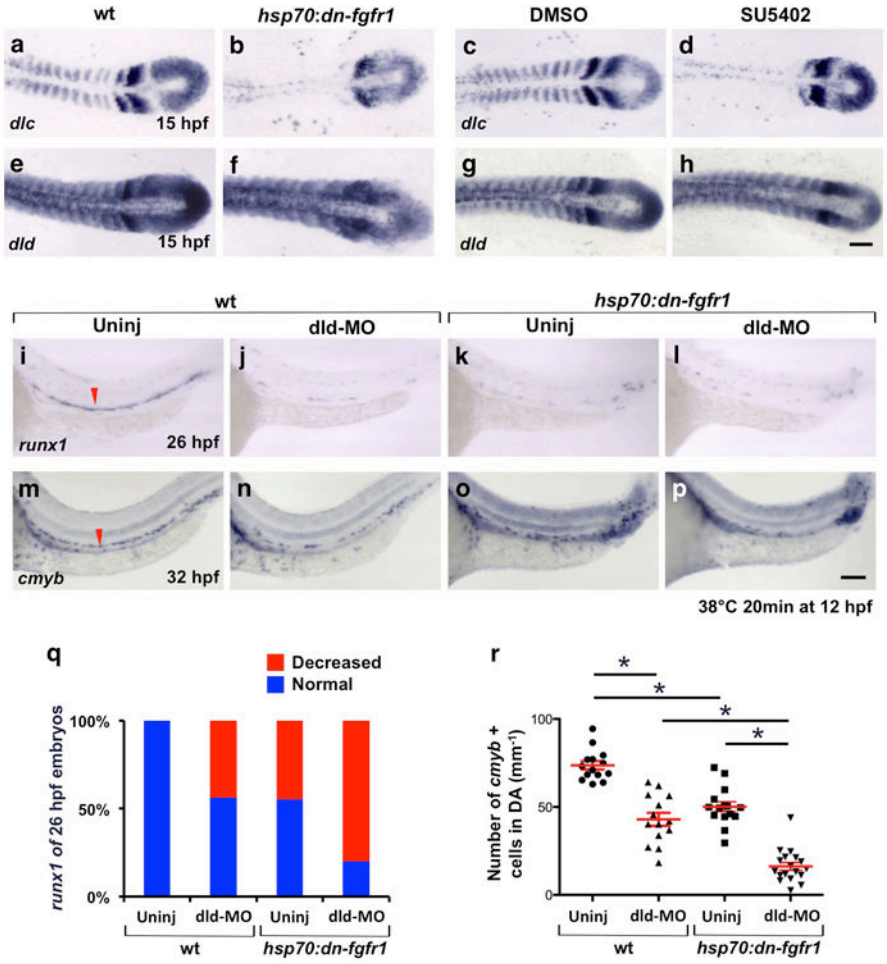

Figure 5. Somitic *dlc* expression, but not *dld*, is regulated by FGF signaling

(**a–h**) Expression of Notch ligands *dlc* and *dld* in 15 hpf *hsp70:dn-fgfr1* animals heat-shocked at 12 hpf compared to wt controls (**a, b, e, f**) and wt embryos incubated with the FGFR-antagonist SU5402 (12 – 15 hpf) compared to DMSO-treated controls (**c, d, g, h**). (**i–p**) Expression of HSC markers *runx1* at 26 hpf (**i–l**) and *cmyb* at 32 hpf (**m–p**) in uninjected wt (**i, m**), dld-MO injected wt (**j, n**), uninjected *hsp70:dn-fgfr1* (**k, o**) and dld-MO injected *hsp70:dn-fgfr1* (**l. p**) embryos heat-shocked at 12 hpf. Red arrowheads indicate *runx1* or *cmyb* WISH signals in uninjected controls (**i, m**). (**q, r**) Percentage of embryos displaying a *runx1* phenotype at 26 hpf (**q**; uninjected wt, n=54; dld-MO injected wt, n=41; uninjected *hsp70:dn-fgfr1*, n=58; dld-MO injected *hsp70:dn-fgfr1*, n=45) and quantification of *cmyb*$^{+}$ cells in DA (**r**; uninjected wt, n=14; dld-MO injected wt, n=14; uninjected *hsp70:dn-fgfr1*, n=15; dld-MO injected *hsp70:dn-fgfr1*, n=18; *mean* ± *s.e.m.*; **P*-value < 0.00001, Student's *t*-test) after blocking *dld* expression and FGF signaling. Scale bars=100μm.

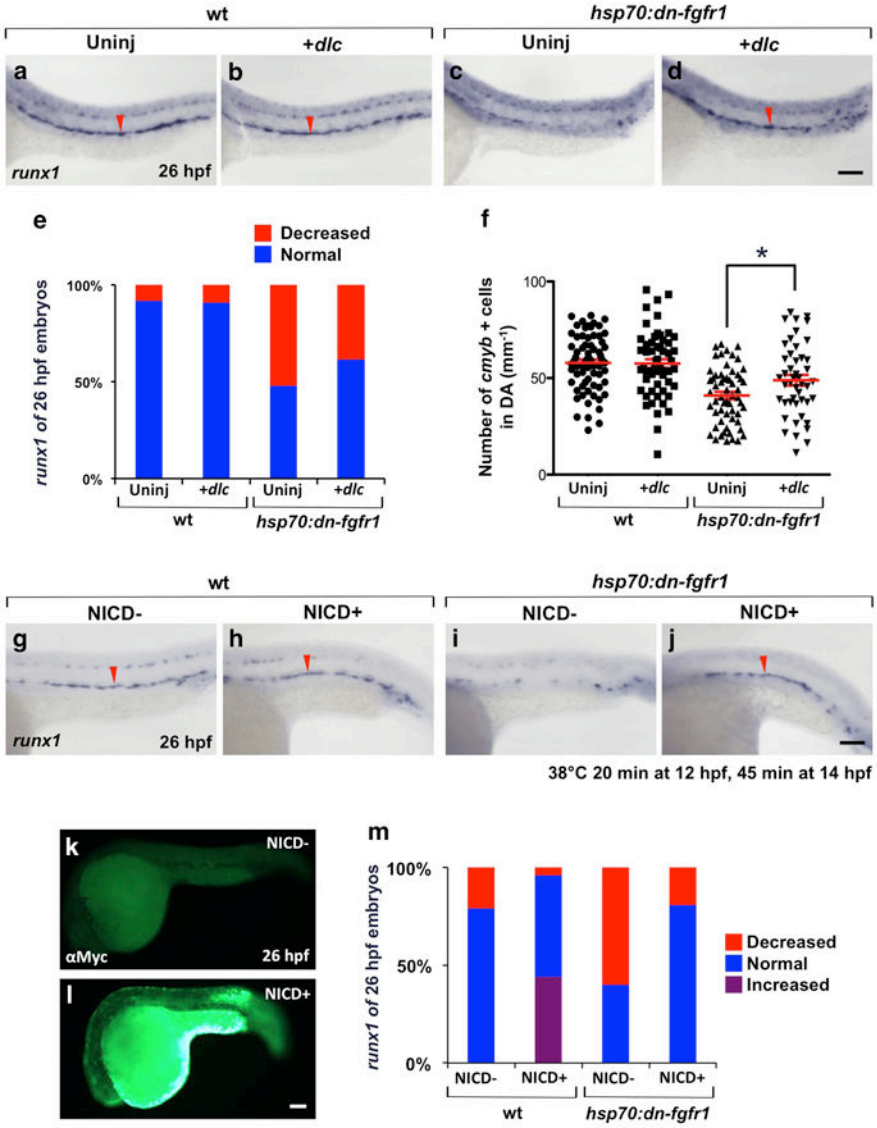

Figure 6. FGF regulation of HSC specification requires the Notch ligand Dlc

(**a–d**) Expression of *runx1* in wt and *hsp70:dn-fgfr1* embryos injected with 100pg of *dlc* mRNA and uninjected controls. Embryos were heat-induced at 12 hpf. (**e, f**) Quantitation of defective embryos showing decreased expression of *runx1* at 26 hpf (**e**; uninjected wt, n=61; *dlc* + wt, n=44; uninjected *hsp70:dn-fgfr1*, n=46; *dlc* + *hsp70:dn-fgfr1*, n=52) and *cmyb*$^{+}$ cells at 32 hpf (**f**; uninjected wt, n=68; *dlc* + wt, n=56; uninjected *hsp70:dn-fgfr1*, n=58; *dlc* + *hsp70:dn-fgfr1*, n=46) using *hsp70:dn-fgfr1* injected with *dlc* mRNA and followed by heat-shock at 12 hpf (*mean* ± *s.e.m.*; **P*-value < 0.05, Student's *t*-test). (**g–j**) *runx1* expression at 26 hpf in *hsp70:gal4; UAS:NICD-myc; hsp70:dn-fgfr1* heat-shocked at both 12 and 14 hpf. (**k, l**) NICD+ embryos were identified by immunostaining for the myc epitope tag, following WISH. (**m**) Percentage of embryos with a *runx1* phenotype at 26 hpf in wt or FGF-blocked, with or without enforced NICD expression (NICD− wt, n=48; NICD + wt, n=25; NICD− *hsp70:dn-fgfr1*, n=20; NICD+ *hsp70:dn-fgfr1*, n=21). Red arrowheads indicate *runx1* expression in the DA. Scale bars=100μm.

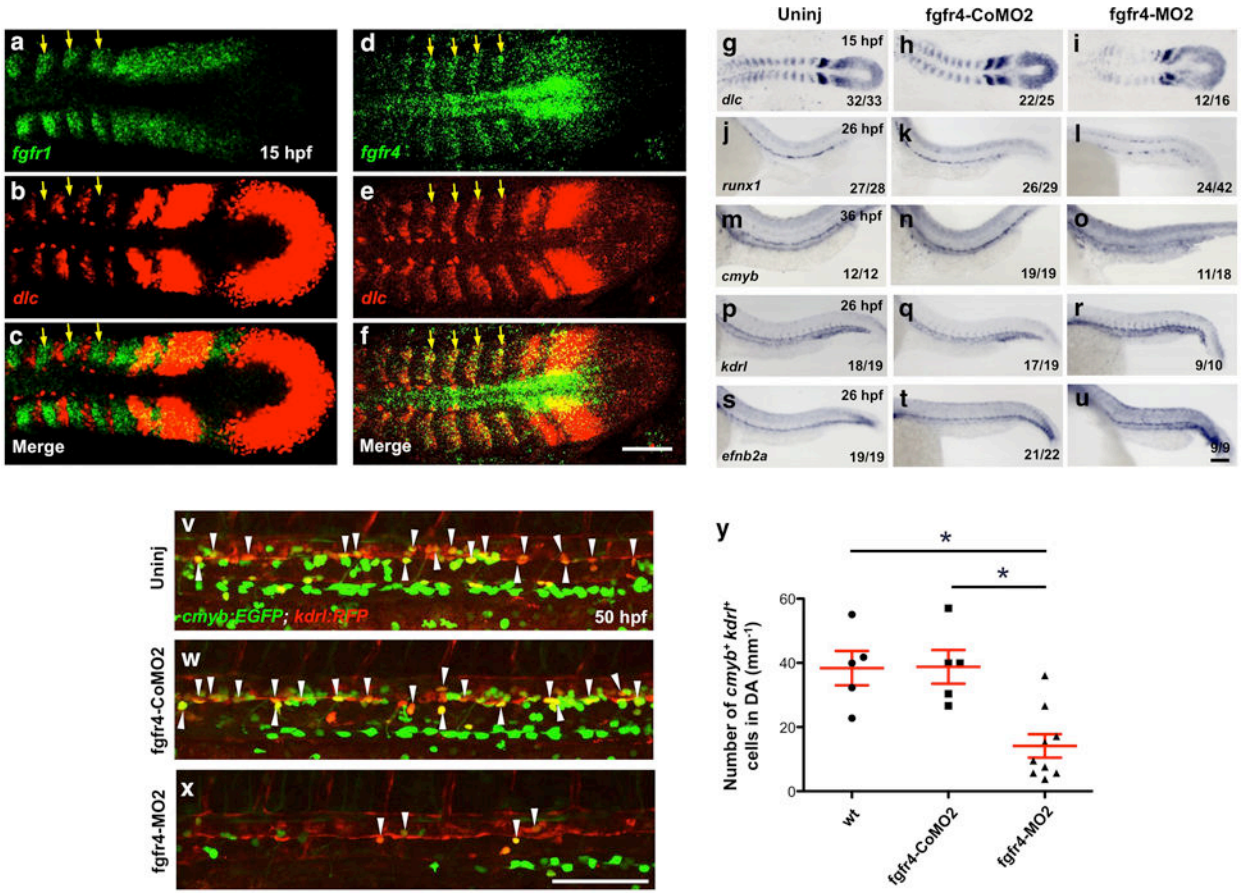

Figure 7. Fgfr4 is required for somitic *dlc* expression and HSC specification

(**a–f**) Single plane confocal images of two-color FISH for *fgfr1* (**a**), *dlc* (**b**) and merged comparison (**c**), and *fgfr4* (**d**), *dlc* (**e**) and their merged comparison (**f**) at 15 hpf. Yellow arrows indicate expressions of *fgfr1* (**a**) or *fgfr4* (**d**) in the somites. (**g–u**) Expression of somitic *dlc* at 15 hpf. (**g–i**), *runx1* at 26 hpf (**j–l**), *cmyb* at 36 hpf (**m–o**), the endothelium marker *kdrl* (**p–r**), and the aortic marker *efnb2a* (**s–u**) at 26 hpf in fgfr4-MO2 injected embryos, compared to uninjected and mismatched control MO (fgfr4-CoMO) injected siblings. (**v–x**) Double-positive HSCs (white arrowheads) in *kdrl:RFP; cmyb:EGFP* transgenics in the fgfr4 morphants (**x**) compared to uninjected (**v**) and mismatched control MO injected (**w**) controls. (**y**) Quantitation of 50 hpf *cmyb*$^{+}$ *kdrl*$^{+}$ double positive HSCs in the DA of fgfr4 morphants (**v–x**) (uninj, n=5; control MO, n=5; fgfr4 morphants, n=9; **P*-value < 0.01, significantly different from uninj and control MO injected ones, Student's *t*-test). Scale bars=100μm.

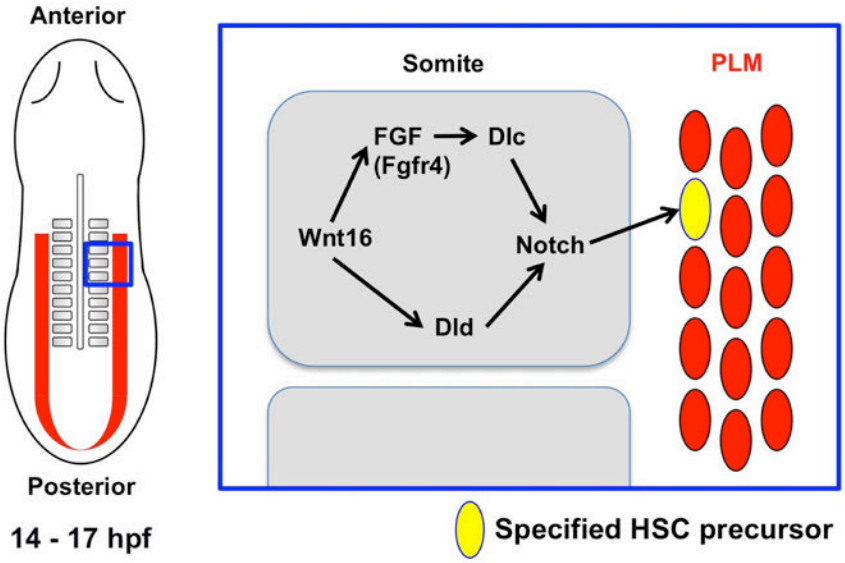

Figure 8. Model of the early FGF requirement in HSC specification

Cartoon depicts a dorsal view during mid-somitogenesis (14 – 17 hpf). FGF signaling specifies HSCs by relaying signals between Wnt16 and Dlc in the somite. Fgfr4 is the key receptor that mediates this Wnt16/Notch HSC specification pathway.